**Cukurova Medical Journal**
ÇUKUROVA ÜNİVERSİTESİ TIP FAKÜLTESİ

Cukurova Med J 2022;47(1):34-43
DOI: 10.17826/cumj.994078

**ARAŞTIRMA / RESEARCH**

# Diagnostic value of diffusion-weighted MRI and conventional MRI in the differentiation of benign and malignant orbital lesions

## Benign ve malign orbital lezyonların ayrımında difüzyon ağırlıklı MRG ve konvansiyonel MRG'nin tanısal değeri

Mesut Öztürk[1], Aslı Tanrıvermiş Sayıt[2], Çetin Çelenk[2], Volkan Yeter[3]

[1]Samsun Gazi State Hospital, Radiology Clinic, Samsun, Turkey
[2]Ondokuz Mayis University Faculty of Medicine, Dept. Radiology, [3]Dept. Ophthalmology, Samsun, Turkey

*Cukurova Medical Journal 2022;47(1):34-43*

**Abstract**

**Purpose:** The aim of this study was to assess the role of diffusion-weighted imaging (DWI) and conventional magnetic resonance imaging (MRI) in the differentiation of benign and malignant orbital lesions.

**Materials and Methods:** 43 patients (27 women and 16 men; mean age: 26.3±28.5) with orbital lesions were assessed with conventional MRI and DWI. The apparent diffusion coefficient (ADC) of the lesions was measured, and maximum ADC ($ADC_{max}$), mean ADC ($ADC_{mean}$), minimum ADC ($ADC_{min}$), the ratio of $ADC_{mean}$ to cerebral white matter ADC ($ADC_{meanratio}$), and the ratio of $ADC_{min}$ to cerebral white matter ADC ($ADC_{minratio}$) were calculated. T1-weighted and T2-weighted imaging features and contrast enhancement patterns were determined. The diagnostic performances of ADC variables and conventional MRI features for the differentiation of benign and malignant orbital lesions were assessed.

**Results:** $ADC_{mean}$, $ADC_{min}$, $ADC_{meanratio}$, and $ADC_{minratio}$ of the malignant lesions were significantly lower than those of the benign ones . $ADC_{meanratio}$ had the highest diagnostic performance with a sensitivity and specificity of 87.5% and 70.4% at a threshold of 1.27. Selecting a cut-off $ADC_{mean}$ of 0.97 × $10^{-3}$ $mm^2/s$ for differentiating benign and malignant lesions revealed 75% sensitivity and 74% specificity. Conventional MRI features were not associated with the malignant diagnosis).

**Conclusion:** ADC values obtained from DWI contribute to the differentiation of benign and malignant orbital lesions.

**Keywords:** Diffusion-weighted imaging; apparent diffusion coefficient; orbital neoplasm; magnetic resonance imaging

**Öz**

**Amaç:** Bu çalışmanın amacı benign ve malign orbital lezyonların ayrımında difüzyon ağırlıklı görüntüleme (DAG) ve konvansiyonel manyetik rezonans görüntüleme (MRG)'nin rolünü değerlendirmektir.

**Gereç ve Yöntem:** Orbital lezyonu 43 hasta (27 kadın ve 16 erkek; ortalama yaş: 26,3 ± 28,5), DAG ve konvansiyonel MRG ile değerlendirildi. Lezyonların görünür difüzyon katsayısı (ADC) ölçüldü ve lezyonların maksimum ADC ($ADC_{maks}$), ortalama ADC ($ADC_{ort}$), minimum ADC ($ADC_{min}$), $ADC_{ort}$ değerinin serebral beyaz cevherin ortalama ADC'sine oranı ($ADC_{ortoran}$) ve $ADC_{min}$'in serebral beyaz cevherin ortalama ADC'sine oranı ($ADC_{minoran}$) hesaplandı. Lezyonların T1 ve T2 ağırlıklı görüntüleme özellikleri ve kontrastlanma paternleri de belirlendi. Malign ve benign orbital lezyonların ayrımı için ADC değişkenlerinin ve konvansiyonel MRG özelliklerinin tanısal performansları değerlendirildi.

**Bulgular:** Malign lezyonların $ADC_{ort}$, $ADC_{min}$, $ADC_{ortoran}$ ve $ADC_{minoran}$ değerleri, benignlerinkinden anlamlı derecede düşüktü. $ADC_{ortoran}$ en yüksek tanısal performansa sahipti; 1,27 sınır değer seçildiğinde duyarlılığı ve özgüllüğü %87,5 ve %70,4 bulundu. Benign ve malign lezyonları ayırt etmek için sınır $ADC_{ort}$ değeri 0,97 × 10-3 $mm^2/s$ seçilmesi, %75 duyarlılık ve %74 özgüllük ortaya çıkardı. Konvansiyonel MRG özellikleri malign tanı ile ilişkili değildi.

**Sonuç:** DAG'den elde edilen ADC değerleri, benign ve malign orbital lezyonların ayrımına katkı sağlamaktadır.

**Anahtar kelimeler**: Difüzyon ağırlıklı görüntüleme, Görünür difüzyon katsayısı, Orbital neoplazi, Manyetik rezonans görüntüleme

Yazışma Adresi/Address for Correspondence: Dr. Mesut Öztürk, Samsun Gazi State Hospital, Radiology Clinic, Ilkadım, Samsun, Turkey. E-mail: dr.mesutozturk@gmail.com
Geliş tarihi/Received: 11.09.2021 Kabul tarihi/Accepted: 24.11.2021

## INTRODUCTION

Orbital lesions are a group of heterogeneous neoplasms that include benign and malignant tumors. The accurate diagnosis of orbital lesions with imaging is crucial for the planning of appropriate surgical treatments and to prevent unnecessary surgical interventions[1,2]. Most orbital lesions do not exhibit typical imaging features in conventional magnetic resonance imaging (MRI), and making the correct diagnosis is often a big challenge[1,3-5]. Anatomic locations and signal characteristics in conventional MRI sequences do not provide enough information to predict malignancy in lesions; therefore, many benign lesions undergo unnecessary biopsies. As the biopsy of periorbital lesions is technically difficult and is associated with a high risk of complications, new non-invasive methods are needed to predict the histological nature of clinically and radiologically indeterminate tumors.

Conventional MRI sequences have been used to evaluate orbital lesions composed of T1-weighted (T1W), T2-weighted (T2W), and contrast-enhanced fat-suppressed T1W images. Although those sequences provide valuable information about the anatomical localization and extension of a lesion, their role in differentiating benign and malignant orbital lesions is limited[6]. Therefore, as in other organ/system tumors, functional imaging sequences, such as diffusion-weighted imaging (DWI), are also used to characterize orbital tumors.

DWI is an MRI-based imaging method that is sensitive to the random Brownian motions of water protons in tissue. DWI has proven to be useful in various organ system diseases and organ tumors[7-10]. Extracellular space is reduced due to hypercellularity, and therefore, lower apparent diffusion coefficient (ADC) values are seen in malignant tumors. DWI has also been reported to play a role in the diagnosis of orbital tumors, and a cut-off ADC value of $1x10^{-3}$ $mm^2/s$ was reported to have high sensitivity and specificity in predicting malignancy[11-19].

Previous studies investigating the role of DWI in the differentiation of benign and malignant orbital tumors used single-slice regions of interest (ROIs) and whole-tumor ROIs to perform ADC measurements[12,15,16]. Both of these ROI selection methods have proven to be effective in lesion differentiation; however, the single-slice ROI method is potentially useful in clinical practice because of its better measurement time, reproducibility, and diagnostic ability[15]. Conversely, several factors, such as magnetic field strength and DWI acquisition parameters, can affect ADC values[13]. Therefore, using internal references, such as cerebral white matter, thalamus, or muscle tissue, may result in better conclusions. However, the number of such studies is very limited in the literature[12,18].

Therefore, the purpose of this study is to investigate the diagnostic value of DWI in the differentiation of malignant and benign orbital lesions. This study uses ADC ratio obtained by the ratio of the lesion ADC to cerebral white matter ADC for an internal standardization purpose. As a secondary aim, the contributions of conventional MRI features in the differentiation of lesions are also investigated.

## MATERIALS AND METHODS

The current study was approved by the Institutional Ethics Committee of the relevant institution (OMU KAEK, 2020/344, 23.02.2021), and the informed consent requirement was waived, as this is a retrospective study. The standards for reporting diagnostic accuracy studies were used[20].

### Study design and patient selection

A retrospective review of the hospital database (Ondokuz Mayis University Hospital) to identify patients who underwent MRI including DWI between January 2017 and December 2019 for the evaluation of an orbital lesion revealed 64 patients. We excluded 11 patients because of low DWI image quality and 10 patients because of unavailable pathological diagnosis or lack of follow-up imaging. As a result, 43 patients with a mean age of $26.3 \pm 28.5$ (range: 0 – 90) were enrolled. There were 16 men (37.2%) and 27 women (62.8%).

The final diagnoses of the lesions were based on histopathological evaluations or typical imaging findings and follow-up imaging. If the lesion underwent surgical resection or biopsy, the results of the histopathological examination were accepted as the final diagnosis. Of the lesions without histopathological examination, those with a stable appearance at 1-year-follow-up or regression with medical treatment and those without metastases in another organ were considered benign. The lesions of patients who had a malignant tumor anywhere in their body and who had a new lesion in the orbit in

the follow-up examination were considered to have metastasized.

## MRI examinations

The MRI examinations of the patients were performed using either a 3T system (Ingenia, Philips Healthcare, Netherlands; n = 13) or two 1.5T systems (Achieva Philips Healthcare, Netherlands; Siemens Magnetom Symphony Quantum, Germany; n = 27 and n = 13, respectively). All patients underwent MRI using a dedicated head coil. In our clinic, the routine MRI protocol applied to patients presenting with a pre-diagnosis of orbital mass is as follows: axial and coronal T2W fat-suppressed spin-echo sequence, sagittal T2W spin-echo sequence, axial T1W spin-echo sequence, axial T1W fat-suppressed spin-echo sequence, and axial and coronal contrast-enhanced fat-suppressed T1W spin-echo sequences. For the contrast-enhanced T1-weighted imaging, gadolinium-based contrast material with a concentration of 0.1 mmol/kg was given intravenously, followed by a 20 cc saline flush.

DWI was obtained in the axial plane using a single-shot spin-echo echo-planar sequence with two b values ($b_0$ = 0, $b_1$ = 1000 s/mm$^2$). Imaging parameters of the DWI sequence in the 3T system were as follows: TR/TE: 1951/88; matrix: 152×106; slice thickness: 3 mm; and field of view: 230×230. The imaging parameters of the DWI sequence in the 1.5T Philips Healthcare system were as follows: TR/TE: 8564/147; matrix: 152×106; slice thickness 3 mm; field of view: 230×230. Imaging parameters of DWI sequence at 1.5T Siemens system were as follows: TR/TE: 3800/99; matrix: 152×106; slice thickness 3 mm; and field of view: 230×230.

## Image evaluation

MRI interpretations were performed by a radiologist (ATS) with six years of experience in head and neck radiology. Image evaluations were performed using the Osirix software for Macintosh (Osirix version 3.8.1, Pixmeo, Switzerland). First, conventional sequences were evaluated, and the anatomic localization of the lesions was noted. Lesions involving intraconal and extraconal spaces, the optic nerve, and the globe were classified as "orbital" lesions. Lesions involving eyelid and preseptal lesions were categorized as "preorbital" lesions. In axial slices, two maximum dimensions of the lesions were measured by drawing two perpendicular lines to each other, and the average of these two values was used in statistical analysis as the mean lesion size. T1W T2W images were evaluated and classified as hypointense or hyperintense according to the cerebral white matter. The contrast enhancement of tumors was also assessed, and the pattern of enhancement was determined if contrast enhancement was present.

For DWI analysis, a single ROI was drawn for tumors less than 1 cm in diameter, and 3 ROIs were drawn for tumors larger than 1 cm (Figure 1 and 2). While drawing the ROIs, distortion artifacts, calcifications, most peripheral regions, and cystic and necrotic areas of the lesions were carefully avoided. The maximum ADC ($ADC_{max}$), mean ADC ($ADC_{mean}$), and minimum ADC ($ADC_{min}$) values of the lesions were calculated. In addition, an ROI was drawn for the cerebral white matter, and the mean ADC ($ADC_{brain}$) value was noted. The ratio of $ADC_{mean}$ to $ADC_{brain}$ ($ADC_{meanratio}$) and the ratio of $ADC_{min}$ to $ADC_{brain}$ ($ADC_{minratio}$) were calculated.

## Statistical analysis

Statistical analysis was performed with SPSS 15.0 for windows. Categorical variables were expressed as frequencies, and continuous variables were expressed as mean and standard deviation (SD) or median and range, as appropriate. The normal distribution of the continuous ADC variables was assessed with the Kolmogorov-Smirnov test. Pearson's chi-squared or Fisher's exact tests were used to compare the gender and conventional MRI features between benign and malignant orbital lesions. The Mann-Whitney U test was used to compare ADC variables between benign and malignant lesions. Student's t test was used to compare patients' ages between benign and malignant lesions. Receiver operating characteristics (ROC) curve analysis was used to assess the diagnostic performance of ADC variables. The optimal cut-off values for each ADC variable were determined by maximizing the Youden index (Youden index = Sensitivity + specificity – 1). Diagnostic performances of the ADC variables were compared with the $ADC_{mean}$ using the McNemar test. For all assessments, a p-value less than 0.05 was indicative of statistical significance.

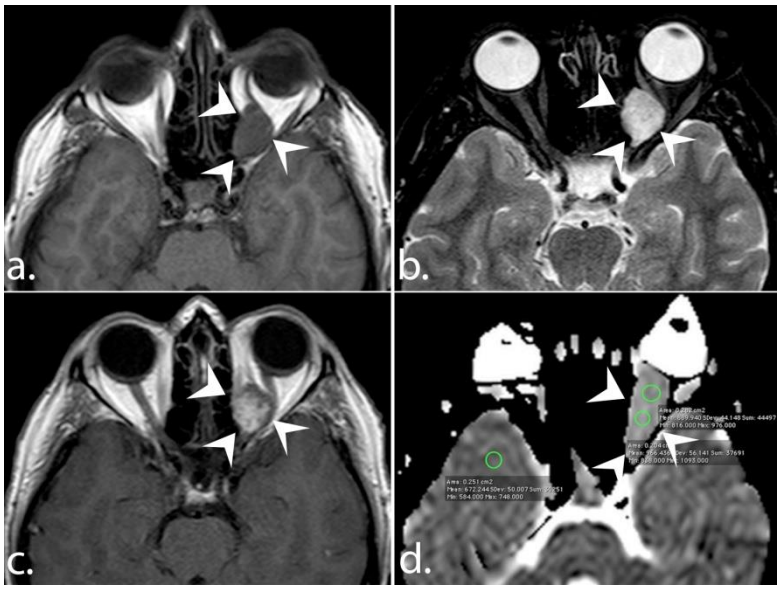


**Figure 1 A 33-year-old male patient with cavernous hemangioma (arrowheads). Axial T1W image (a) demonstrates a hypointense lesion in the extraconal space of the left orbital. The lesion is hyperintense in the fat-suppressed T2W image (b). Contrast-enhanced T1W sequence (c) demonstrates the heterogeneous enhancement of the lesion. ADC map (d) shows the ADC measurement of the tumor.**

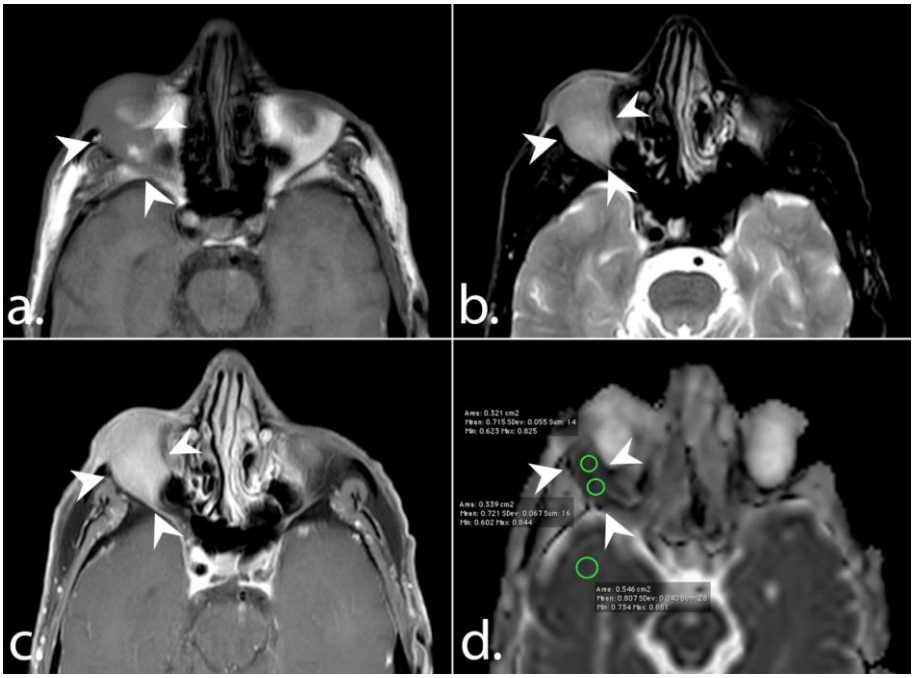


**Figure 2. A 72-year-old male patient with non-Hodgkin's lymphoma (arrowheads). Axial T1W image (a) demonstrates a hypointense lesion in the extraconal space of the left orbital. The lesion is hyperintense in the fat-suppressed T2W image (b). Contrast-enhanced T1W sequence (c) demonstrates homogenous enhancement of the lesion. ADC map (d) shows ADC measurement of the tumor.**

## RESULTS

The demographic data of the study population are shown in Table 1. There were 27 benign (62.7%) and 16 malignant (37.3%) tumors. Their final diagnoses are shown in Table 2. Fourteen tumors were located in the preorbital region, whereas 29 tumors were located in the orbital region. Of the orbital tumors, 13 were located in the extraconal region, 4 were located in the intraconal region, 6 were located in the optic nerve, and 3 were located in the globe. Three tumors were located both in the extraconal and intraconal regions. Lesion localization was not associated with the malignant diagnosis (p = 0.416).

**Table 1. Demographic data of the study population**

| Data | Whole population (n = 43) | Benign lesions (n = 27) | Malignant lesions (n = 16) | p value |
|---|---|---|---|---|
| Mean age (years) | 26.3 ± 28.5 | 14.9 ± 18.8 | 45.6 ± 32.2 | <0.001 |
| Mean diameter (mm) | 19.3 ± 8.7 | 17.0 ± 6.1 | 23.2 ± 11.0 | 0.022 |
| Gender (n) | | | | 0.534 |
| Male | 16 (37.2%) | 11 (68.8%) | 5 (31.3%) | |
| Female | 27 (62.8%) | 16 (59.3%) | 11 (40.7%) | |
| Localization (n) | | | | 0.416 |
| Preorbital | 14 (32.6%) | 10 (71.4%) | 4 (28.6%) | |
| Intraorbital | 29 (67.4%) | 17 (58.6%) | 12 (41.4%) | |

**Table 2. Diagnosis of the lesions**

| Benign lesions (n = 27) | Malignant lesions (n = 16) |
|---|---|
| Miscellaneous benign (n = 19) | Lymphoma (n = 2) |
| Hemangioma (n = 4) | High-grade undifferentiated carcinoma (n = 2) |
| Menengioma (n = 1) | Rhabdomyosarcoma (n = 2) |
| Dermoid cyst (n = 1) | Malignant melanoma (n = 2) |
| Chronic inflammation (n = 1) | Metastasis (n = 3) |
| Pilocytic astrocytoma (n = 1) | Squamous cell carcinoma (n = 2) |
| | Neuroendocrine tumor (n = 1) |
| | Low-grade mesenchymal tumor (n = 1) |
| | Immature teratoma (n = 1) |

**Table 3. Conventional MRI features of the benign and malignant orbital tumors.**

| Variable | Benign | Malignant | p value |
|---|---|---|---|
| T1W image appearance | | | 1.000 |
| Hyperintense | 4 (57.1%) | 3 (42.9%) | |
| Hypointense | 23 (63.9%) | 13 (36.1%) | |
| T2W image appearance | | | 0.133 |
| Hyperintense | 27 (65.9%) | 14 (34.1%) | |
| Hypointense | 0 (0%) | 2 (100%) | |
| Contrast enhancement | | | 0.283 |
| Present | 21 (60%) | 14 (40%) | |
| Absent | 3 (100%) | 0 (0%) | |
| Contrast enhancement pattern | | | 1.000 |
| Homogenous | 14 (60.9%) | 9 (39.1%) | |
| Heterogeneous | 7 (58.3%) | 5 (41.7%) | |

T1W: T1 weighted, T2W: T2 weighted

Patients with benign tumors were significantly younger than patients with malignant tumors (14.9 ± 18.8 vs. 45.6 ± 32.2, p < 0.001). In terms of gender distribution, there was no statistically significant difference between benign and malignant tumors (p = 0.534). The mean diameter of the benign tumors

was significantly smaller than that of the malignant tumors (p = 0.022). T1W imaging appearance, T2W imaging appearance, presence of contrast enhancement, and contrast enhancement pattern were not associated with the pathological diagnosis (Table 3).Differences in ADC values between benign and malignant tumors are shown in Table 4 and Figure 3 as box-plot graphs. The median $ADC_{mean}$ of the malignant tumors ($0.99 \times 10^{-3}$ $mm^2/s$) was significantly lower than that of the benign tumors ($1.23 \times 10^{-3}$ $mm^2/s$, p = 0.012). There was no statistically significant difference between the median $ADC_{max}$ of the malignant and benign lesions (1.25 vs. $1.67 \times 10^{-3}$ $mm^2/s$, p = 0.059). The median $ADC_{min}$ of the malignant tumors ($0.67 \times 10^{-3}$ $mm^2/s$) was significantly lower than that of the benign tumors ($0.85 \times 10^{-3}$ $mm^2/s$, p = 0.021). Median $ADC_{meanratio}$ of the malignant tumors (1.12) was significantly lower than that of the benign tumors (1.44, p = 0.008). The median $ADC_{minratio}$ of the malignant tumors (0.84) was significantly lower than that of the benign tumors (1.08, p = 0.022).

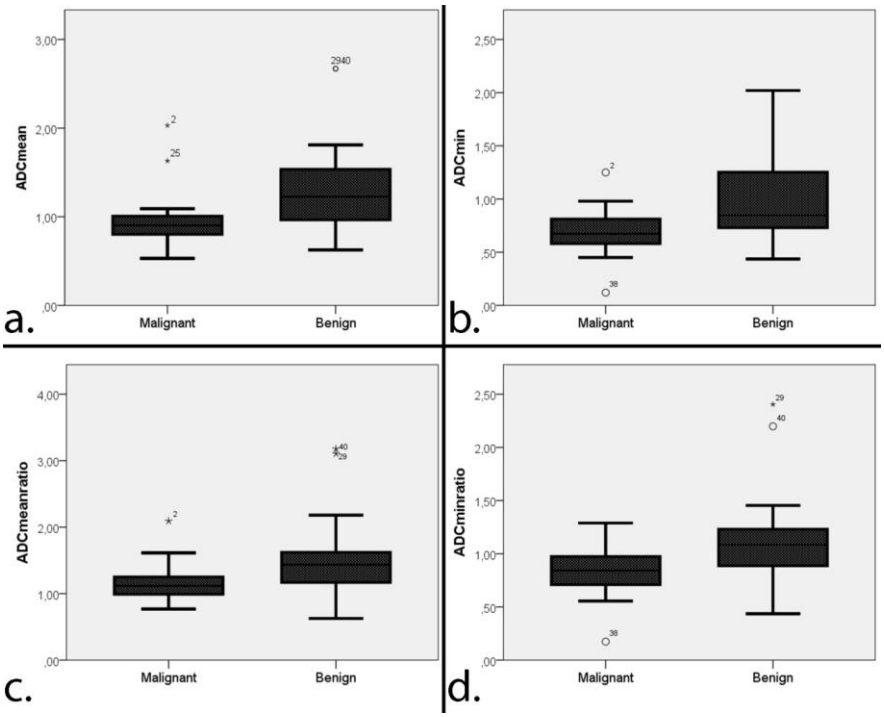


**Figure 3. Box-and-whisker plots show the comparison of $ADC_{mean}$ (a), $ADC_{min}$ (b), $ADC_{meanratio}$ (c), and $ADC_{minratio}$ (d) between benign and malignant tumors.**

**Table 4. Differences in ADC values between malignant and benign lesions**

| Variable | Benign lesions (n = 27) | Malignant lesions (n = 16) | p value |
|---|---|---|---|
| $ADC_{mean}$ | 1.23 (0.63 – 2.67) | 0.99 (0.53 – 2.03) | 0.012 |
| $ADC_{max}$ | 1.67 (0.76 – 3.13) | 1.25 (0.81 – 3.24) | 0.059 |
| $ADC_{min}$ | 0.85 (0.44- 2.02) | 0.67 (0.12 – 1.25) | 0.021 |
| $ADC_{meanratio}$ | 1.44 (0.63 – 3.18) | 1.12 (0.77 – 2.09) | 0.008 |
| $ADC_{minratio}$ | 1.08 (0.44 – 2.40) | 0.84 (0.17 – 1.29) | 0.022 |

Numbers are expressed as medians, and ranges are in the parentheses; $ADC_{mean}$: mean apparent diffusion coefficient; $ADC_{max}$: maximum apparent diffusion coefficient; $ADC_{min}$: minimum apparent diffusion coefficient; $ADC_{meanratio}$: the ratio of the mean apparent diffusion coefficient of the orbital lesion to the apparent diffusion coefficient of cerebral white matter; $ADC_{minratio}$: The ratio of the minimum apparent diffusion coefficient of the orbital lesion to the apparent diffusion coefficient of cerebral white matter.

Diagnostic performances of ADC measurements in the differentiation of benign and malignant tumors are shown in Table 5 and Figure 4. $ADC_{meanratio}$ had the highest diagnostic performance (area under curve [AUC]: 0.743, 95% confidence interval [CI]: 0.585 – 0.902, p = 0.008), followed by $ADC_{mean}$ (AUC: 0.731, 95% CI: 0.569 – 0.894, p = 0.012). An optimal cut-off $ADC_{meanratio}$ was 1.27, and it revealed 87.5% sensitivity and 70.4% specificity. A cut-off $ADC_{mean}$ value lesser than $0.97 \times 10^{-3}$ $mm^2/s$ for diagnosing a malignant tumor led to sensitivity and specificity values of 75% and 74%, respectively. ROC analysis of $ADC_{min}$ for the differentiation of malignant and benign tumors revealed an AUC of 0.713 (CI: 0.558 – 0.868, p = 0.021). The sensitivity and specificity values were found to be 62.5% and 77.8% for an optimal cut-off of $0.72 \times 10^{-3}$ $mm^2/s$. The diagnostic performance of $ADC_{mean}$ was not significantly different from the diagnostic performances of the $ADC_{min}$, $ADC_{meanratio}$ and $ADC_{minratio}$ (p = 0.375, p = 0.453, and p = 0.070, respectively).

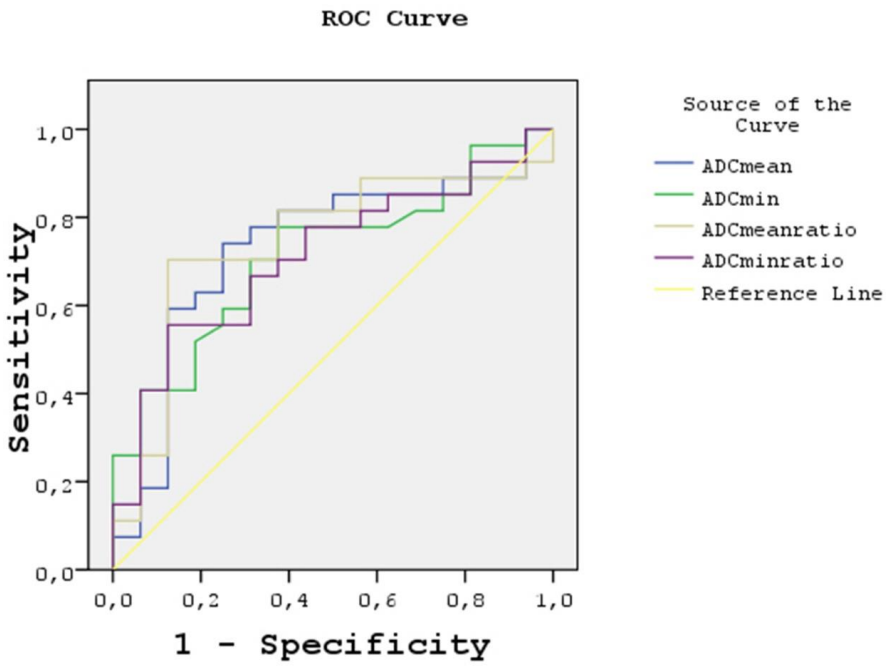


**Figure 4. ROC curves for $ADC_{mean}$, $ADC_{min}$, $ADC_{meanratio}$, and $ADC_{minratio}$. Highest AUCbelonged to $ADC_{meanratio}$ (AUC: 0.743) followed by $ADC_{mean}$ (AUC: 0.731).**

**Table 5. Diagnostic performances of ADC measurements in the differentiation of benign and malignant orbital lesions.**

| Variable | Cut-off | Sensitivity | Specificity | AUC | $p^a$ | $p^b$ |
|---|---|---|---|---|---|---|
| $ADC_{mean}$ | 0.97 | 75.0% | 74.0% | 0.731 (0.569 – 0.894) | 0.012 | |
| $ADC_{min}$ | 0.72 | 62.5% | 77.8% | 0.713 (0.558 – 0.868) | 0.021 | 0.375 |
| $ADC_{meanratio}$ | 1.27 | 87.5% | 70.4% | 0.743 (0.585 – 0.902) | 0.008 | 0.453 |
| $ADC_{minratio}$ | 1.00 | 87.5% | 55.6% | 0.711 (0.554 – 0.867) | 0.022 | 0.070 |

[a]: derived from diagnostic performance analysis; [b]: derived from the comparison of the diagnostic performance of $ADC_{mean}$ with other ADC variables; $ADC_{mean}$: mean apparent diffusion coefficient; $ADC_{min}$: minimum apparent diffusion coefficient; $ADC_{meanratio}$: the ratio of the mean apparent diffusion coefficient of the orbital lesion to the apparent diffusion coefficient of cerebral white matter; $ADC_{minratio}$: the ratio of the minimum apparent diffusion coefficient of the orbital lesion to the apparent diffusion coefficient of cerebral white matter; AUC: area under curve.

## DISCUSSION

Our study results confirmed that DWI is useful in differentiating benign and malignant orbital tumors. Benign tumors were significantly more common in younger patients, and they were significantly smaller in diameter compared to malignant ones. Conventional imaging features were not significantly different between benign and malignant orbital tumors.

In this study, $ADC_{mean}$ and $ADC_{min}$ of malignant tumors were significantly lower than those of benign ones. This condition can be attributed to the hypercellularity of malignant tumors. The distance between cells becomes smaller with the increasing number of cells, and the free diffusion of water molecules is restricted. Restricted diffusion causes low numerical values in ADC maps.

Sepahdari et al.[12] evaluated 47 patients with orbital tumors using DWI and concluded that malignant lesions had significantly lower ADC values than benign tumors. In their study, a cut-off value of 1.0 × $10^{-3}$ $mm^2/s$ led to 63% sensitivity and 84% specificity. Our optimal cut-off value (0.97 × $10^{-3}$ $mm^2/s$) was also similar to that in their study. They also calculated the ratio of the ADC of the lesion to the ADC of white matter and found an optimal cut-off value of 1.2, which is quite similar to ours. In another study evaluating the diagnostic performance of DWI in the pediatric population by Jaju et al., mean ADC and lesion ADC-to-thalamus ADC ratios were found to be useful for the differentiation of benign orbital tumors[18]. In their study, the mean ADC cut-off value of 1.14 × $10^{-3}$ $mm^2/s$ provided a sensitivity of 84% and a specificity of 100%, while an ADC ratio of 1.4 provided a sensitivity of 81% and specificity of 89%. In other studies by different authors, ADC values of malignant lesions were also found to be lower than the ADC values of benign lesions[12,16,21–23]. In these studies, the optimal ADC cut-off values were found to be in the ranges of 0.84 and 1.15 × $10^{-3}$ $mm^2/s$. Our mean ADC cut-off value was 0.97 × $10^{-3}$ $mm^2/s$, which is consistent with the previous literature.

Xu et al.[24] evaluated the diagnostic performances of three different ROI selection methods, including whole-tumor, single-slice, and reader-defined small samples, for the measurement of ADC values of orbital tumors. The authors did not find a statistically significant difference between the diagnostic performances of these three methods; however, the single-slice technique was reported to be useful in clinical practice, as its measurement time and repeatability were better. In our study, we also used the single-slice method.

DWI and ADC values can be affected by the magnetic field strength, coil system, imaging parameters, and different manufacturers. In our study, MRI examinations of the patients were performed using three different MRI systems. For this reason, besides measuring the ADC values of the lesions, we also calculated the ratio of the lesion ADC to the normal white matter ADC. In this way, we tried to generate an internal reference point and thereby eliminate the MRI machines' variability. Our study results revealed that the ratio of lesion ADC to white matter ADC is effective in differentiating malignant and benign tumors, and it has been shown to have similar diagnostic performance to conventional single-slice ADC measurements.

This study has several limitations. First, we included a relatively small number of patients. More studies with larger populations are needed to validate our results. Second, the patients included in our study covered a wide range of age groups, including infants, children, and adults. Third, most of the benign diagnoses were based on radiological and clinical findings, and we lacked true histopathological diagnoses. Fourth, a very heterogeneous tumor group involving different compartments of the orbit was included in the study. Fifth, the diagnoses of the lesions were composed of a very wide range of tumors and tumor-like lesions. Sixth, the evaluation of contrast enhancement characteristics was based on the visual analysis of static T1W images, and therefore, small and slowly enhancing lesions may be misinterpreted as non-enhanced. Seventh, we used different MRI systems to acquire the images, and we used the ADC ratios to overcome this limitation. Finally, image interpretation was performed by only one radiologist experienced in head-neck imaging, and interobserver and intraobserver variability were not assessed.

In conclusion, our study showed that DWI can differentiate benign and malignant orbital tumors. Conventional imaging features, including T1W and T2W image signals and contrast enhancement features, were not useful in the differentiation.

**Yazar Katkıları:** Çalışma konsepti/Tasarımı: MÖ, ATS, CC, VY; Veri toplama: MÖ, ATS, CC, VY; Veri analizi ve yorumlama: MÖ, ATS, CC, VY; Yazı taslağı: MÖ, ATS, CC, VY; İçeriğin eleştirel incelenmesi: MÖ, ATS, CC, VY; Son onay ve sorumluluk: MÖ, ATS, CC, VY; Teknik ve

malzeme desteği: MÖ, ATS, CC, VY; Süpervizyon: MÖ, ATS, CC, VY; Fon sağlama (mevcut ise): yok.
**Etik Onay:** Bu çalışma için Ondokuz Mayıs Üniversitesi Klinik Araştırmalar Etik Kurulundan 23.02.2021 tarih ve 2020-344 sayılı kararı ile etik onay alınmıştır.
**Hakem Değerlendirmesi:** Dış bağımsız.
**Çıkar Çatışması:** Yazarlar çıkar çatışması beyan etmemişlerdir.
**Finansal Destek:** Yazarlar finansal destek beyan etmemişlerdir.

**Author Contributions:** Concept/Design : MÖ, ATS, CC, VY; Data acquisition: MÖ, ATS, CC, VY; Data analysis and interpretation: MÖ, ATS, CC, VY; Drafting manuscript: MÖ, ATS, CC, VY; Critical revision of manuscript: MÖ, ATS, CC, VY; Final approval and accountability: MÖ, ATS, CC, VY; Technical or material support: MÖ, ATS, CC, VY; Supervision: MÖ, ATS, CC, VY; Securing funding (if available): n/a.
**Ethical Approval:** For this study, ethical approval was obtained from the Ethics Committee of Ondokuz Mayıs University Clinical Research Council with the decision dated 23.02.2021 and numbered 2020-344.
**Peer-review:** Externally peer-reviewed.
**Conflict of Interest:** Authors declared no conflict of interest.
**Financial Disclosure:** Authors declared no financial support

## REFERENCES

1. Goh PS, Gi MT, Charlton A, Tan C, Gangadhara Sundar JK, Amrith S. Review of orbital imaging. Eur J Radiol. 2008;66:387–95.
2. Tailor TD, Gupta D, Dalley RW, Keene CD, Anzai Y. Orbital neoplasms in adults: clinical, radiologic, and pathologic review. Radiographics. 2013;33:1739–58.
3. Hu H, Xu X-Q, Liu H, Hong X-N, Shi H-B, Wu F-Y. Orbital benign and malignant lymphoproliferative disorders: Differentiation using semi-quantitative and quantitative analysis of dynamic contrast-enhanced magnetic resonance imaging. Eur J Radiol. 2017;88:88–94.
4. Lemke AJ, Kazi I, Felix R. Magnetic resonance imaging of orbital tumors. Eur Radiol. 2006;16:2207–19.
5. Ben Simon GJ, Annunziata CC, Fink J, Villablanca P, McCann JD, Goldberg RA. Rethinking orbital imaging establishing guidelines for interpreting orbital imaging studies and evaluating their predictive value in patients with orbital tumors. Ophthalmology. 2005;112:2196–207.
6. Xian J, Zhang Z, Wang Z, Li J, Yang B, Man F et al. Value of MR imaging in the differentiation of benign and malignant orbital tumors in adults. Eur Radiol. 2010;20:1692–702.
7. Bekci T, Polat AV, Aslan K, Tomak L, Ceyhan Bilgici M, Danaci M. Diagnostic performance of diffusion-weighted MRI in the diagnosis of ovarian torsion: comparison of torsed and nonaffected ovaries. Clin Imaging. 2016;40:1029–33.
8. Aslan S. Added value of contrast-enhanced and diffusion-weighted MRI data sets for characterization of perianal fistulas; single center experience. Artic Ann Med Res. 2020;27:2763–71.
9. Wang J, Takashima S, Takayama F, Kawakami S, Saito A, Matsushita T et al. Head and neck lesions: characterization with diffusion-weighted echo-planar MR imaging. Radiology. 2001;220:621–30.
10. Vandecaveye V, De Keyzer F, Vander Poorten V, Dirix P, Verbeken E, Nuyts S et al. Head and neck squamous cell carcinoma: value of diffusion-weighted MR imaging for nodal staging. Radiology. 2009;251:134–46.
11. Politi LS, Forghani R, Godi C, Resti AG, Ponzoni M, Bianchi S et al. Ocular adnexal lymphoma: diffusion-weighted mr imaging for differential diagnosis and therapeutic monitoring. Radiology. 2010;256:565–74.
12. Sepahdari AR, Aakalu VK, Setabutr P, Shiehmorteza M, Naheedy JH, Mafee MF. Indeterminate orbital masses: restricted diffusion at MR imaging with echo-planar diffusion-weighted imaging predicts malignancy. Radiology. 2010;256:554–64.
13. Haradome K, Haradome H, Usui Y, Ueda S, Kwee TC, Saito K et al. Orbital lymphoproliferative disorders (OLPDs): value of MR imaging for differentiating orbital lymphoma from benign OPLDs. AJNR Am J Neuroradiol. 2014;35:1976–82.
14. Xu XQ, Hu H, Su GY, Zhang L, Liu H, Hong XN et al. Orbital indeterminate lesions in adults: combined magnetic resonance morphometry and histogram analysis of apparent diffusion coefficient maps for predicting malignancy. Acad Radiol. 2016;23:200–8.
15. Xu XQ, Hu H, Su GY, Liu H, Hong XN, Shi HB et al. Utility of histogram analysis of ADC maps for differentiating orbital tumors. Diagn Interv Radiol. 2016;22:161–7.
16. Razek AAKA, Elkhamary S, Mousa A. Differentiation between benign and malignant orbital tumors at 3-T diffusion MR-imaging. Neuroradiology. 2011;53:517–22.
17. Xu XQ, Hu H, Liu H, Wu JF, Cao P, Shi HB et al. Benign and malignant orbital lymphoproliferative disorders: differentiating using multiparametric MRI at 3.0T. J Magn Reson Imaging. 2017;45:167–76.
18. Jaju A, Rychlik K, Ryan ME. MRI of pediatric orbital masses: role of quantitative diffusion-weighted imaging in differentiating benign from malignant lesions. Clin Neuroradiol. 2020;30:615–24.
19. Maldonado FR, Princich JP, Micheletti L, Toronchik MS, Erripa JI, Rugilo C. Quantitative characterization of extraocular orbital lesions in children using diffusion-weighted imaging. Pediatr Radiol. 2021;51:119-127.
20. Bossuyt PM, Reitsma JB, Bruns DE, Gatsonis CA, Glasziou PP, Irwig L et al. STARD 2015: an updated list of essential items for reporting diagnostic accuracy studies. Radiology. 2015;277:826–32.
21. Sasaki M, Yamada K, Watanabe Y, Matsui M, Ida M, Fujiwara S et al. Variability in absolute apparent diffusion coefficient values across different platforms may be substantial: a multivendor, multi-institutional comparison study. Radiology. 2008;249:624–30.
22. Şerifoğlu İ, Oz İİ, Damar M, Tokgöz Ö, Yazgan Ö, Erdem Z. Diffusion-weighted imaging in the head and neck region: usefulness of apparent diffusion

coefficient values for characterization of lesions. Diagn Interv Radiol. 2015;21:208–14.
23. Fatima Z, Ichikawa T, Ishigame K, Motosugi U, Waqar AB, Hori M et al. Orbital masses: the usefulness of diffusion-weighted imaging in lesion categorization. Clin Neuroradiol. 2014;24:129–34.
24. Xu XQ, Hu H, Su GY, Liu H, Shi HB, Wu FY. Diffusion weighted imaging for differentiating benign from malignant orbital tumors: diagnostic performance of the apparent diffusion coefficient based on region of interest selection method. Korean J Radiol. 2016;17:650–6.